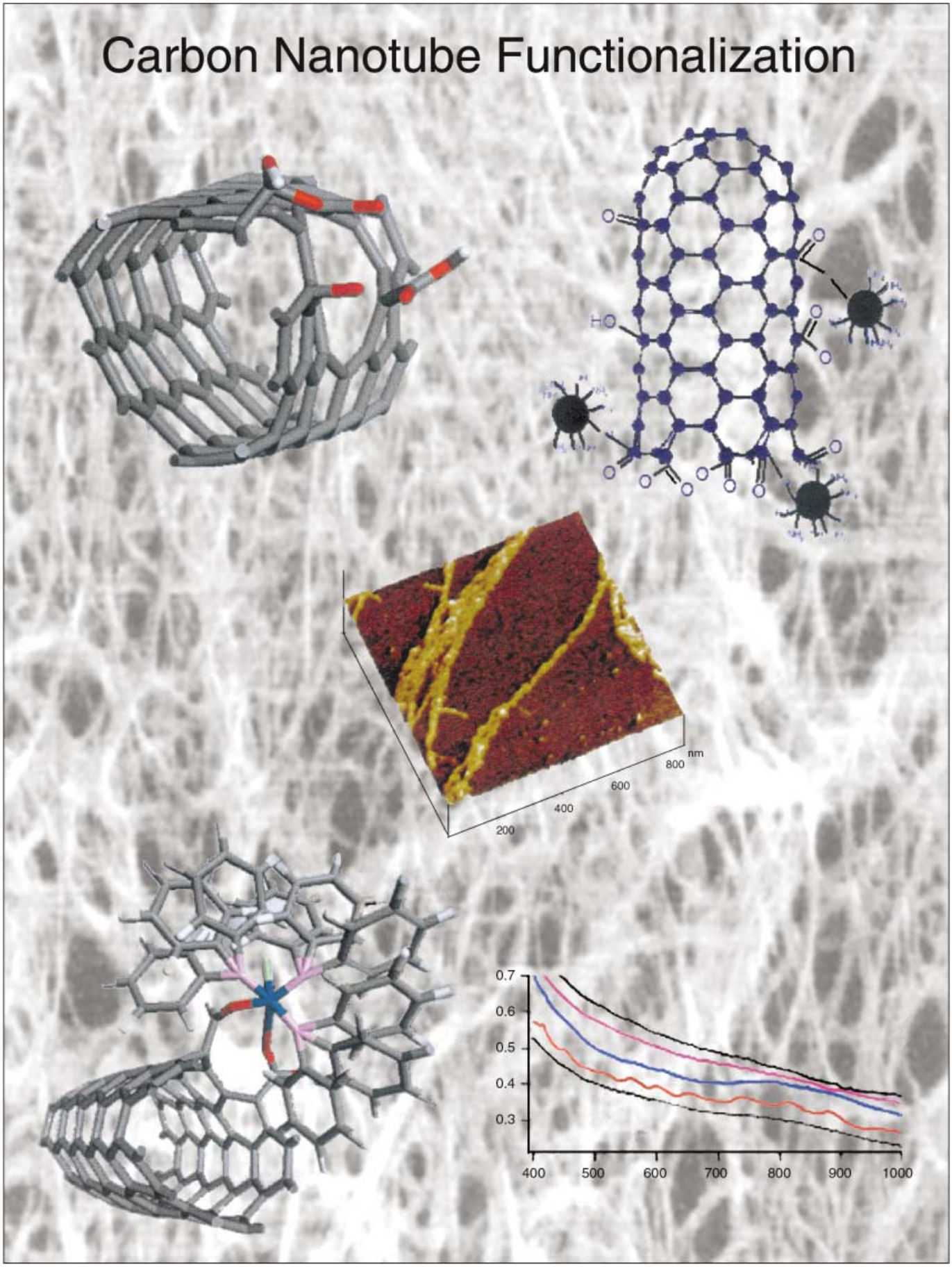

DOI: 10.1002/chem.200204618 *Chem. Eur. J.* **2003**, *9*, 1898 – 1908

Rational Chemical Strategies for Carbon Nanotube Functionalization

Sarbajit Banerjee,[a] Michael G. C. Kahn,[a] and Stanislaus S. Wong*[a, b]

Abstract: Whereas the chemistry of fullerenes is well-established, the chemistry of single-walled carbon nanotubes (SWNTs) is a relatively unexplored field of research. Investigations into the bonding of moieties onto SWNTs are important because they provide fundamental structural insight into how nanoscale interactions occur. Hence, understanding SWNT chemistry becomes critical to rational, predictive manipulation of their properties. Among the strategies discussed include molecular metal complexation with SWNTs to control site-selective chemistry in these systems. In particular, work has been performed with Vaska's and Wilkinson's complexes to create functionalized adducts. Functionalization should offer a relatively simple means of tube solubilization and bundle exfoliation, and also allows for tubes to be utilized as recoverable catalyst supports. Solubilization of oxidized SWNTs has also been achieved through derivatization by using a functionalized organic crown ether. The resultant adduct yielded concentrations of dissolved nanotubes on the order of 1 $g L^{-1}$ in water and at elevated concentrations in a range of organic solvents, traditionally poor for SWNT manipulation. To further demonstrate chemical processability of SWNTs, we have subjected them to ozonolysis, followed by treatment with various independent reagents, to rationally generate a higher proportion of oxygenated functional groups on the nanotube surface. This protocol has been found to purify nanotubes. More importantly, the reaction sequence has been found to ozonize the sidewalls of these nanotubes. Finally, SWNTs have also been chemically modified with quantum dots and oxide nanocrystals. A composite heterostructure consisting of nanotubes joined to nanocrystals offers a unique opportunity to obtain desired physical, electronic, and chemical properties by adjusting synthetic conditions to tailor the size and structure of the individual sub-components, with implications for self-assembly.

Keywords: nanostructures · nanotechnology · nanotubes · ozonolysis · synthesis design

Introduction

The whole principle of rational synthesis and characterization at the nanoscale relies on the ability to generate chemically well-defined building blocks with tailorable properties. Indeed, the dramatic growth in nanoscience research over the last decade or so has been fuelled largely by advances in the predictive synthesis, processing, and characterization of nanoscale systems, including nanocrystals, nanoparticles, nanotubes, and nanorods. Ideally, the net result of nanoscale chemical design is the production of structures that achieve monodispersity, stability, and crystallinity with a predictable morphology. Most importantly, their chemical composition should be intrinsically definable. Many of the synthetic methods used to attain these aforementioned goals have been based on principles derived from semiconductor technology, solid-state chemistry, and molecular inorganic cluster chemistry. Recently, in this context, a lot of effort in our group has been expended on rationally and predictably modifying the chemical properties of carbon nanotubes, by using similar types of strategies.

Single-walled carbon nanotubes (SWNTs),[1] in particular, have been at the forefront of novel nanoscale investigations due to their unique structure-dependent electronic and mechanical properties.[2–5] They are thought to have a host of wide-ranging, potential applications, for example, as catalyst supports in heterogeneous catalysis, field emitters, high-strength engineering fibers, sensors, actuators, tips for scanning probe microscopy, gas storage media, and as molecular wires for the next generation of electronics devices.[6–15] The combination of the helicity and diameter of SWNTs, defined by the roll-up vector, often determines whether a tube is a metal or a semiconductor. Moreover, the mechanical strength (i.e. buckling force) of a tube is a function of its length and diameter. SWNTs have been synthesized in our laboratory, in gram quantities, by means of a chemical vapor deposition process. Indeed, the advantage of SWNTs is that they are chemically, molecularly defined structures with reproducible dimensions.

[a] Prof. S. S. Wong, S. Banerjee, M. G. C. Kahn
Department of Chemistry
State University of New York at Stony Brook
Stony Brook, NY 11794 (USA)
Fax: (+1) 631-632-7960
E-mail: sswong@notes.cc.sunysb.edu

[b] Prof. S. S. Wong
Materials and Chemical Sciences Department
Brookhaven National Laboratory, Building 480
Upton, NY 11973 (USA)
Fax: (+1) 631-344-4071
E-mail: sswong@bnl.gov

 DOI: 10.1002/chem.200204618

Understanding the chemistry of SWNTs is critical to rational manipulation of their properties. Chemical modification is essential for the deposition of catalysts and other species onto nanotube surfaces for nanocatalytic and sensor applications. Moreover, such studies are crucial for oriented assembly of these nanostructures. The ability to disperse and solubilize carbon nanotubes would also open up new prospects in aligning and forming molecular devices. Nonetheless, this objective necessitates controlled chemical functionalization of tubes, a relatively unexplored area of research, compared with, for instance, fullerene chemistry.

From a fundamental scientific perspective, functionalization allows for the exploration of the intrinsic molecular nature of these SWNTs and permits studies at the rich, structural interface between true molecules and bulk materials. In general, chemical modification strategies have targeted SWNT defects, end caps, and sidewalls, as well as the hollow interior.[16–18] Representative approaches to derivatization include covalent chemistry of conjugated double bonds within the SWNT,[19–21] noncovalent π-stacking,[22] covalent interactions at dangling functionalities at nanotube ends and defects,[23] and wrapping of macromolecules.[24–26] Chemical functionalization of SWNTs attached to conventional atomic force microscopy probes has also been demonstrated as a methodology of yielding high-resolution, chemically sensitive images on samples that contain multiple chemical domains.[27, 28] In this last case, functionalization occurred at the end of these nanotubes, often involving only a few molecules.

We have focused on more generalized, holistic approaches aimed at understanding the inorganic and organic molecular chemistry of SWNTs, not only at the ends but also at the sidewalls and defect sites as well. As an example, we have used solution-phase ozonolysis as a methodology not only of derivatizing nanotube sidewalls, but also, coupled with additional, carefully chosen reagents, as a means of introducing specific oxygenated functional groups in a targeted manner.

Indeed, the theme of our research has been to treat nanotubes as chemical reagents (be it inorganic or organic) in their own right. From their inherent structure, one can view nanotubes as sterically bulky, π-conjugated ligands or conversely, as electron-deficient alkenes. As such, there are a number of issues we have been interested in. Firstly, what types of bonding interactions govern the formation and stability of adducts between nanotubes and other molecular species? Secondly, what type of correlation exists between reactivity and the intrinsic structure (i.e. diameter and length) of these tubes? Thirdly, can the degree of functionalization in these materials be controlled? Fourthly, do the resulting functionalized adducts have unique properties and applications? Hence, the work in our laboratory has been involved with understanding chemical reactivity involving SWNTs from a structural and mechanistic perspective; this should hopefully expand the breadth and types of reactions SWNTs can undergo in the solution phase. Moreover, controllable chemical functionalization suggests that the unique electronic and mechanical properties of SWNTs can be tailored in a determinable manner.

To this end, we will describe a number of different techniques for rational chemical derivatization of carbon nanotubes including molecular coordination involving metal complexes, organic derivatization with crown ethers, solution-phase ozonoloysis, and functionalization with quantum dots and metal oxide nanocrystals. The salient points of all of this work are summarized as follows:

1) Predictive chemical coordination to nanotubes is possible by using conventional molecular organic and inorganic methodologies.
2) There are differences in reactivity between fullerenes and nanotubes.
3) The resulting functionalized nanotube adducts possess unique physical (such as optical), catalytic, and electronic properties.

To understand and verify the presence and extent of chemical derivatization, we have employed a whole host of physicochemical techniques, ranging from NMR and IR spectroscopy to electron and atomic force microscopy (AFM) to facilitate structural characterization.

Solubilization of tubes through chemical functionalization has also been a key objective of our studies.[23] Indeed, it is essential not only for reproducible nanoscale solution chemistry and, subsequently, reliable photophysical analyses, but also for chromatographic purification[29, 30] and the directed assembly of tubes.[31] It has been proposed, for instance, that large organic groups assist in solubility by exfoliation of the bundles into individual tubes through the formation of intervening moieties that can overcome the intrinsic van der Waals forces[32] between these tubes. Whereas solubilization has been achieved in water, with functionalization methodologies involving glucosamine[33] and gum arabic,[34] as well as in common organic solvents, by using thionyl chloride and octadecylamine, in this article, we generalize these results by noting that practically all of our strategies discussed for chemical derivatization yield greatly improved solubilization of tubes, often in solvents generally considered to be poor media for SWNTs. Moreover, it has also been noted that functionalization appears to have the complementary effect of selectively solubilizing specific subsets or sub-populations of tubes.

Derivatization with Metal-Containing Molecular Coordination Complexes

Metal coordination constitutes a very significant component of the crystal-engineering repertoire. One strategy that we have been exploring is to derivatize SWNTs with relatively bulky inorganic complexes; this not only yields a novel metal-based molecular coordination complex, but also offers the possibility of tailorable solubility in a variety of solvents, through mechanisms such as charge-mediated stabilization and ligand exchange along the length of the tube, without completely disrupting the tube's electronic structure. In addition, these generated adducts can be used in a number of different catalytic processes, including homogeneous catalysis, upon which the expensive metal-support assembly can be facilely recovered from solution.

SWNT/Vaska's complex adduct: Specifically, both oxidized nanotubes and raw, unfunctionalized SWNTs have been

treated with Vaska's compound *trans*-[IrCl(CO)(PPh_3)$_2$] to form covalent nanotube–metal complexes.[35] This functionalization process not only opens up the area of metallo-organic chemistry to SWNTs, but also suggests potential applications in catalysis and molecular electronics.

Moreover, the complexes of oxidized SWNTs with Vaska's compound are much more soluble in DMF than raw tubes, a finding that should facilitate chemical manipulation as well as photophysical analyses of these materials. In fact, the solubility of oxidized tubes varied with the concentration of Vaska's complex added, suggesting that dissolution was chemically induced. The solubility of a typical adduct sample in DMF at room temperature was $\sim 250\,mg\,L^{-1}$, about an order of magnitude improvement over that found for unmodified tubes.[32]

Results were confirmed by ^{31}P NMR, FT-IR, and electron ionization mass spectroscopy, as well as data from transmission electron microscopy (TEM) and energy dispersive X-ray analysis (EDX). In effect, it is theorized that the unoxidized tubes are likely to coordinate as an electron deficient alkene in an η^2 manner. As evidence, the upshift in the carbonyl band IR stretching frequency observed is a measure of the electron density at the metal center and suggests electron deficiency of the SWNT double bond. Whereas for the oxidized tubes, the previous mechanism is a possibility, it is reasonable to expect that the coordination is more likely to occur through the oxygen atoms coating the nanotube exterior. That is, oxidative addition is the more plausible option, considering that the outer surface of the tubes is oxygenated, particularly at ends and defect sites, and that the Ir complex is extremely susceptible to this type of addition. One potential mechanism would involve carbonyl groups *ortho* to each other on a benzenoid ring that could add to the metal to generate a complex with an *ortho*-diolato ligand.[36]

Interactions of SWNTs with this iridium complex highlight some of the differences of SWNT chemistry with respect to that of fullerenes. For instance, although both SWNTs and fullerenes are characterized by a nonplanar sp^2 configuration, curvature effects and different degrees of local strain between the two structures introduce substantial differences in reactivity. Specifically, the presence of five-membered cyclopentadienyl-like rings in C_{60} substantially enhances the affinity of (6,6) bonds in coordinating metal complexes. However, theoretical calculations on molecular fragments replicating SWNT surface curvature indicate that, unlike in the case of fullerenes, five-membered rings are not present to stabilize π^* ligand orbitals and, hence, backbonding interactions are much weaker in these systems.[37] This would rationalize the preference for oxidative addition, when that should become a possibility. In fact, in the electronic spectra (Figure 1), the disappearance of an intense peak at 389 nm, distinctive for Vaska's complex, is considered as a diagnostic for the conversion of Ir^{I} to Ir^{III};[38] this is exactly what we have found with our SWNT adducts. The spectrum of oxidized nanotubes is featureless in this region.

We note other differences in the mechanism of reactivity between SWNTs and fullerenes. As a further example, the additive chemistry of fullerenes is well-developed,[39, 40] whereas that of SWNTs is less understood. It is postulated that the conformational strain, relieved in addition reactions involving fullerenes, originates in its intrinsic pyramidalization,[41] whereas for SWNTs, the pyramidalization effect is not as acute and is, in fact, secondary to the more critical π-orbital misalignment[42] between adjacent pairs of conjugated carbon atoms.[18, 43] As this last effect scales with diameter, we expect chemical reactivity in SWNTs to provide an opportunity with which to achieve diameter-selective resolution and separation,[44] since smaller diameters of tubes are very extensively strained and, hence, have very high π-orbital misalignment angles. As a consequence, we predict that the smallest diameter tubes recently isolated (~ 4 Å)[45] will show identical or increased reactivity with respect to that of fullerenes. Specifically, we postulate that reactions involving the direct, low-temperature addition of halogen atoms or the cycloaddition of fused aromatic systems, which have not as yet been observed for the traditional diameter ranges (6–17 Å) of SWNTs, should be doable by using these smaller sized tubes.

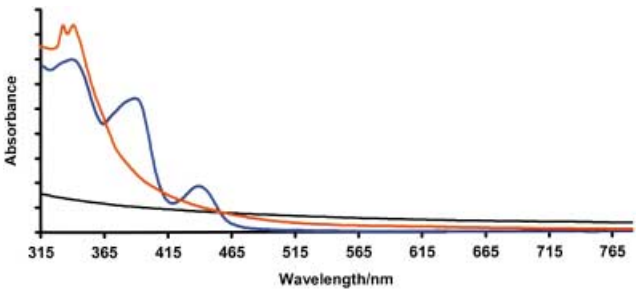

Figure 1. UV-visible spectra of functionalized nanotube adducts. Vaska's complex (blue), oxidized SWNTs (black), and SWNT-Vaska's adduct (red).

SWNT/Wilkinson's adduct: Oxidized carbon nanotubes have also been treated, under an argon atmosphere, with another metal-containing molecular complex, namely Wilkinson's compound, [RhCl(PPh_3)$_3$]. It has been found that the Rh metal coordinates to these nanotubes through the increased number of oxygen atoms, forming a hexacoordinate structure around the Rh atom (Figure 2).[46] In this section, we discuss the implications of inorganic functionalization of these tubes on the subsequent solubilization, exfoliation, selective derivatization, and catalysis involving these adducts.

Solubilization: In terms of solubility, it has been found that low concentrations of Wilkinson's complex are sufficient to dissolve large amounts of the SWNT material. The adduct also shows a comparatively high degree of solubility in DMSO, reproducibly $>150\,mg\,L^{-1}$, and up to as much as $250\,mg\,L^{-1}$. Reasonable solubility values (roughly 30% of that noted in DMSO) of functionalized tubes have been noted in DMF and THF, which are generally considered to be poor to moderate solvents for underivatized SWNTs.[47, 48] The fact that the tubes can be precipitated out upon the addition of a high ionic strength solution suggests that the tubes are charged to some extent in solution, possibly through the role of counterions to our complexes, and that solubility observed occurs by means of electric double-layer stabilization.

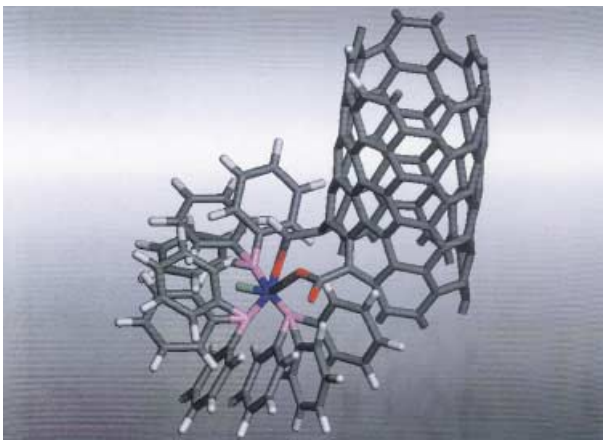

Figure 2. Schematic respresntation of the SWNT–$[RhCl(PPh_3)_3]$ adduct. The figure shows a possible mode of coordination, whereby oxygenated functionalities, such as a carboxylic acid group and a keto group depicted here, at the opened ends of a (5,5) SWNT are able to coordinate to the metal center. Oxygenated functionalities are expected to be present at ends and defect sites.

Exfoliation: Another important consequence of functionalization is the observed, chemically-induced exfoliation of larger tubular bundles into smaller aggregates. Indeed, electron microscopy (Figure 3) and AFM data (Figure 4) of the derivatized adducts indicate a high density of small bundles, of the order of 15–20 nm in diameter (as compared with 30 nm on average for unfunctionalized tubes) and up to a few microns in length, as well as individual tubes, arising from separation of larger bundles. It is predicted that molecules of the bulky inorganic complex spread along the length of the SWNT, lead to disruption of the intrinsic intertube van der Waals interactions, and thereby enable these small tubular bundles to stay apart in solution in an analogous manner in which bulky organic groups and polymers do so.[34, 49, 50]

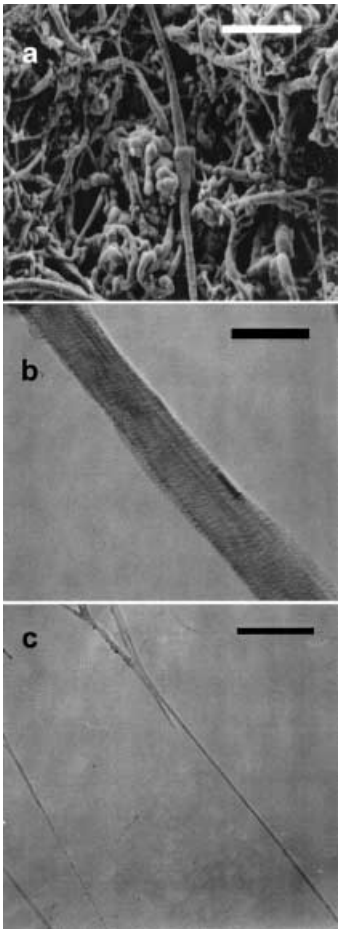

Figure 3. a) Scanning electron micrograph (SEM) of pristine, as-prepared nanotube bundles. Scale bar represents 700 nm. b) TEM of a purified SWNT bundle. The scale bar denotes 30 nm. c) TEM image showing exfoliation of nanotubes functionalized with Wilkinson's complex into smaller bundles and individual tubes. Scale bar represents 30 nm.

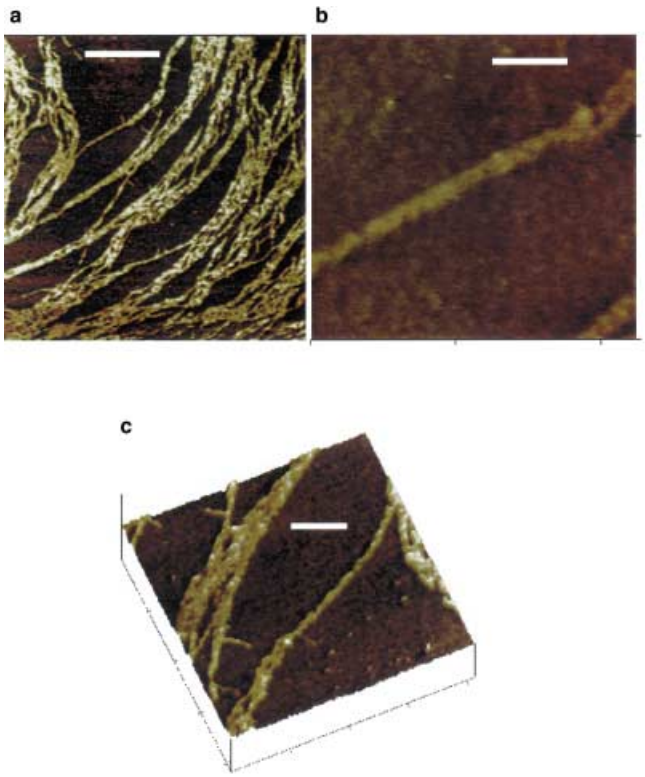

Figure 4. Atomic force microscopy (AFM) height images of functionalized nanotube adducts. Scale bars are a) 500 nm, b) 100 nm, and c) 200 nm, respectively. a) A high density of tubes has been deposited from solution. Aggregates of tubes appear to be exfoliating into smaller bundles. b) Image of a single bundle roughly 15 nm in diameter. c) A 3D view of exfoliating tubes. The bundles are relatively clean and free of nanoparticulate impurities.

Selectivity: The functionalization process may also select for the presence of distributions of smaller diameter tubes. Indeed, the NIR spectrum (Figure 5a) of the functionalized adduct shows some clear differences to that of the raw nanotube sample. Of particular significance is the presence of substructure and greater resolution of some of these peaks in the adduct spectrum, whereby only broad, unresolved humps had been seen for the raw, underivatized nanotubes. Because the width of the features in the NIR spectrum originates from the overlap of whole aggregate transitions from all tubes present of different diameters and helicities, the greater spectral resolution of peaks observed suggests that certain discrete diameter distributions of nanotubes may be preferentially solubilized as a direct consequence of chemical functionalization.[48, 51]

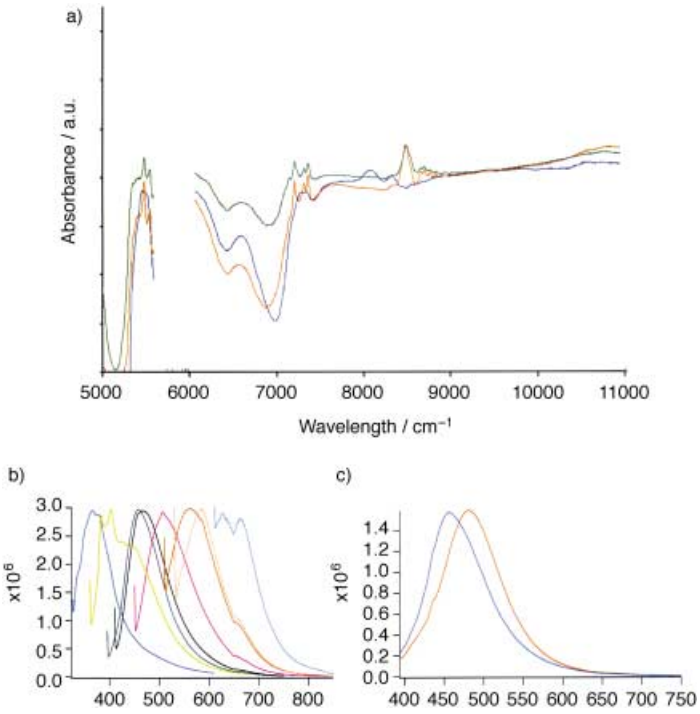

Figure 5. a) NIR spectra of pristine nanotubes (blue) and functionalized SWNT/Wilkinson's complex adduct in DMSO. Spectra of a saturated SWNT/Wilkinson's adduct solution (red) as well as a dilution of this solution (green) are shown. The area of the spectrum omitted consists of strong solvent absorbances. b) Photoluminescence emission spectra of functionalized nanotubes in DMSO solution upon excitation at 315, 350, 385, 400, 440, 500, 520, and 600 nm (from left to right). Note the excitation wavelength dependence of the emission maxima. Emission spectra show fine structure on excitation at < 385 nm. The emission peaks and presence of shoulders in the band in the 600–700 nm region correspond to band gap emission from metallic SWNTs. c) Emission spectra upon 385 nm excitation for functionalized SWNT/Wilkinson's complex adduct solution in DMSO, and diluted with acetone (blue) and methanol (red).

In other words, there is evidence of a degree of size and diameter selectivity, associated with the derivatization reaction and accompanying solubilization process. Since the interband transition energy is inversely proportional to the tube diameter,[5, 52, 53] these data are indicative of preferential, selective derivatization and dissolution of smaller diameter tubes, as a result of functionalization; this would be expected based on our earlier discussion of SWNT reactivity. The other implication is that functionalization may have the effect of slightly narrowing down the overall distribution of diameters in the sample, namely by skewing it towards smaller tubes; this would also lead to the higher spectral resolution observed. The photoluminescence spectrum (Figure 5b) shows band-gap photoluminescence from metallic tubes; this is complementary to the band-gap fluorescence recently reported for semiconducting tubes,[50] and presents good evidence that individual SWNTs are indeed being probed in solution.

Catalysis: Finally, an important consideration for the design of these adducts, in particular, has been their practical utility and efficiency in catalyzing chemical reactions. SWNTs have been used in the past as supports in heterogeneous catalysis.[7, 8] Functionalized SWNT/Wilkinson's complex adducts have been found to catalyze the hydrogenation of alkenes (e.g., cyclohexene) to alkanes (e.g., cyclohexane) at room temperature. To the best of our knowledge, this represents the first example of a homogeneous catalysis reaction demonstrated with a nanotube support.

This is significant because in more sophisticated reactions, the metal–support interactions in these functionalized nanotube adducts may provide a means of controlling the selectivity (such as the geometry and, potentially, even the chirality) of the resultant product distribution. We are currently investigating and optimizing the kinetics and mechanism of catalysis mediated by functionalized nanotube adducts.

Our further experiments with other metal-containing complexes suggests that, in general, square-planar complexes are ideal for functionalizing SWNTs. Indeed, the tendency of Ir and Rh complexes to undergo oxidative addition onto SWNTs is further enhanced by the presence of accommodating ligands, such as dicarboxylate-like moieties. It is substantially more challenging to coordinate complexes with bulky ligands (and hence, more sterically hindered binding pockets) onto tubes. A crystal-engineering approach to linking nanotubes by metal complexes by using similar principles has recently been reported.[54]

Derivatization with Organic Moieties

To generalize and broaden the potential of functionalization, we have also solubilized oxidized SWNTs through the attachment of organic moieties in a large number of solvents of varying polarity.[55] In this case, we attached a functionalized organic crown ether, namely 2-aminomethyl[18]crown-6, to our SWNTs. The resultant adduct yielded concentrations of dissolved nanotubes on the order of $\sim 1\ \mathrm{g\,L^{-1}}$ in water as well as in methanol, according to optical measurements. These values are dramatic improvements over conventional dissolution behavior of unfunctionalized nanotubes. The nanotube/crown ether adduct can be readily redissolved in a number of different organic solvents (Table 1), such as ethanol, 2-propanol, acetone, *o*-dichlorobenzene (ODCB), dimethylformamide (DMF), tetrahydrofuran (THF), dimethylsulfoxide (DMSO), ethyl acetate, and benzene at substantially high concentrations. One implication of these results lies in further exploitation of the solution chemistry of these tubes for photophysical analyses in a number of previously untested solvents as well as for the generation of novel nanoscale architectures.

Table 1. The solubility of crown ether functionalized SWNTs in different solvents of varying polarity.

Solvent	Concentration of SWNTs in solution [$\mathrm{mg\,L^{-1}}$]
THF	270
acetone	280
DMSO	290
ODCB	300
DMF	610
water	1100
methanol	1600

Because the reaction conditions are too mild for amide formation and, moreover, as the adduct does not appear to form in the presence of standard carbodiimide linker reagents, the structures of these adducts are likely to be a consequence of a noncovalent, zwitterionic chemical interaction between carboxylic groups on the oxidized tubes and amine moieties attached to the sidechain of the crown ether derivative (Figure 6).

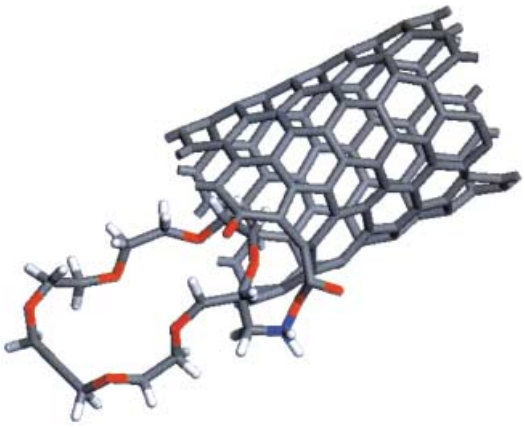

Figure 6. Optimized geometry for crown ether functionalized (5,5) SWNTs. Adduct formation likely arises from a zwitterionic interaction between the carboxylic acid groups on the SWNT and the amino functionality on the derivatized crown ether.

Derivatization with Solution-Phase Ozonoloysis

Oxidative processes used to purify nanotubes are capable of generating a variety of oxygenated functional groups, such as aldehydic, ketonic, alcoholic, and carboxylic moieties, at the nanotube ends and, in particular, at structural defect sites along the tube walls etched by the oxidizing agent. What has not been readily determined is the number, distribution, and location of these generated oxygenated functional groups. Addressing this issue would aid in achieving rational spatial and molecular control over the extent of chemical derivatization in nanotubes.

We have developed an ozonolysis protocol (Figure 7) that involves treatment of nanotubes at $-78\,^{\circ}C$, followed by reaction with various reagents, in independent runs, to generate a higher proportion of carboxlyic acid/ester, ketone/aldehyde, and alcohol groups on the nanotube surface.[56] This "one-pot" oxidative methodology has three major consequences: firstly, the purification of as-prepared SWNTs to obtain a high-quality product (Figure 8); secondly, the chemical functionalization of nanotube sidewalls; and thirdly, a systematic procedure to select for particular distributions of oxygenated functional groups in the resultant purified SWNTs.

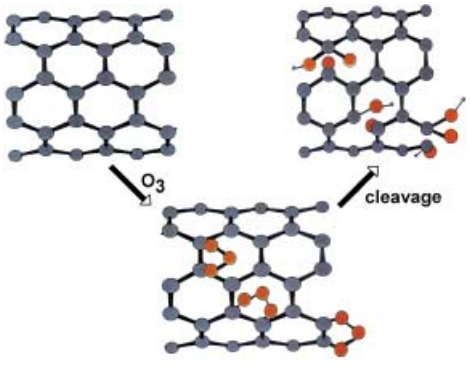

Figure 7. Schematic represenation of a section of the sidewall of an armchair SWNT. Upon treatment with ozone, a proposed intermediate, namely a primary ozonide, forms. Cleavage of the ozonide with appropriate chemical agents can yield a range of different functional groups. As examples, the presence of aldehydic, ketonic, alcoholic, and carboxylic groups are schematically illustrated.

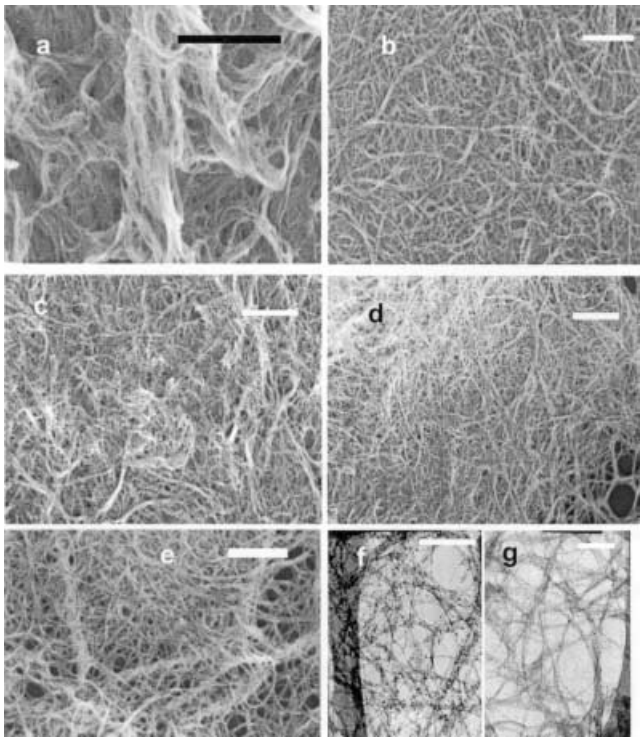

Figure 8. SEMs of a number of ozonized SWNT samples. a) Raw, as-prepared HiPco tubes. b) Ozonized sample without further processing. c) Sample after $NaBH_4$ treatment. d) Sample after cleavage with DMS. e) Sample after processing with H_2O_2. Scale bars for these micrographs are 1 μm in each case. Transmission electron micrographs of f) as-prepared HiPco SWNTs and g) SWNTs after an ozonolysis and HCl treatment. Scale bars are 130 and 140 nm, respectively.

The last goal is accomplished by generating higher proportions of carboxylic acids, aldehydes/ketones, and alcohols on the surfaces of carbon nanotubes through chemical treatment with hydrogen peroxide (H_2O_2), dimethyl sulfide (DMS), and sodium borohydride ($NaBH_4$), respectively; this takes advantage of the high reactivity of primary ozonides, which are presumed to form upon the ozonolysis of SWNT dispersions in solution (Table 2).

It should be stressed that the protocol described, at the moment, cannot generate 100% abundance of a particular oxygenated functional group. One of the main reasons for not obtaining such favorable selectivity is that the unstable ozonide intermediate may rapidly quench (especially in solution),[57] form high yields of secondary ozonides, or even react with any remaining contaminants, such as Fe impurities. All of these secondary processes provide for competing

Table 2. Percentages of surface functional, oxygenated groups obtained from curve fitting of the C_{1s} peaks of the SWNT HiPco samples subjected to ozonolysis in methanol at $-78\,^{\circ}C$, followed by selective chemical treatments.

Sample	C−O species (alcohol)	C=O species (aldehyde/ketone)	O−C=O species (carboxylic acid/ester)
ozonized tubes.	13.3	50.8	35.9
ozonized tubes treated with H_2O_2.	37.0	9.4	53.6
ozonized tubes treated with DMS.	28.7	41.1	30.2
ozonized tubes treated with $NaBH_4$.	29.1	36.3	34.6

pathways and, hence, lead to different product distributions from the full conversion values expected.

H_2O_2 treatment yields greater than 50% carboxylic acid functionalities, the predominant group in that set of data. These results are a clear improvement over conventional nanotube processing procedures, which include Ar^+ ion sputtering[58] and permanganate oxidation,[59] whereby the percentage of carboxylic groups is $<15\%$. The large alcohol content arises from a H_2O_2–iron-particle interaction, which can form reactive secondary hydroxyl radicals. Similarly, it is evident that $NaBH_4$ is an appropriate and logical reagent for generating almost 30% of alcoholic species, comparable to the best results obtained by thermal treatment in air and ion sputtering.[58] Likewise, use of DMS led to a reasonable yield of over 40% of keto groups, the highest amongst all of the workup reagents tried. To note the effectiveness of ozonolysis, as a comparison, unprocessed, pristine SWNTs, from a variety of sources, frequently possess percentages of oxygenated −C−O, −C=O, and −COOH functionalities under 10%.[60]

While generating other oxygenated functional groups solely by ozonide cleavage is rather difficult, and while not all of the major issues are fully resolved, our data provide for a promising and rational strategy and foundation with which to approach this very challenging problem of controlling functional group distributions on nanotube surfaces. These results are important, because, traditionally, much of SWNT chemistry has focused on exploiting the reactivity of the oxygenated functional groups at defect sites and end caps. Ozonolysis provides a means of generalizing this chemistry to nanotube sidewalls and surfaces, especially important for high-surface-area applications.

Derivatization with Nanocrystals and Quantum Dots

A novel strategy of altering the electronic properties of nanotubes is to chemically functionalize them with a moiety or structure whose intrinsic properties are themselves structurally and electronically configurable. One such structure is the family of semiconductor nanocrystals,[61] such as CdS and CdSe, alternately known as quantum dots, which exhibit strongly size-dependent optical and electrical properties. The high luminescence yield of these materials[62] as well as the potential of adjusting emission and absorption wavelengths by selecting for nanocrystal size make quantum dots attractive for constructing optoelectronic devices, for instance, with tailored properties. In fact, the electronic structure of semiconductor nanocrystallites exhibits distinctive quantum effects;[63] the bandgap of these materials increases with decreasing particle size.

One of the major goals behind designing semiconductor–metal composite nanoscale heterostructures is to influence the energetics and interfacial charge-transfer processes in a favorable manner. To this effect, we have reported the synthesis and characterization of SWNTs covalently joined to CdSe and TiO_2 semiconductor nanocrystals by short-chain organic molecule linkers.[64] In each case, purified, oxidized nanotubes were reacted with nanocrystals, derivatized with either amine or acid terminal groups in a reaction mediated by a carbodiimide reagent (Figure 9). By judiciously varying the nature of the organic capping groups on the nanocrystal surface and the organic bifunctional linkers, we can modulate interactions between the nanotubes and the nanocrystals, with implications for self-assembly. Based on electronic absorption spectroscopy, charge transfer is thought to proceed from the nanocrystal

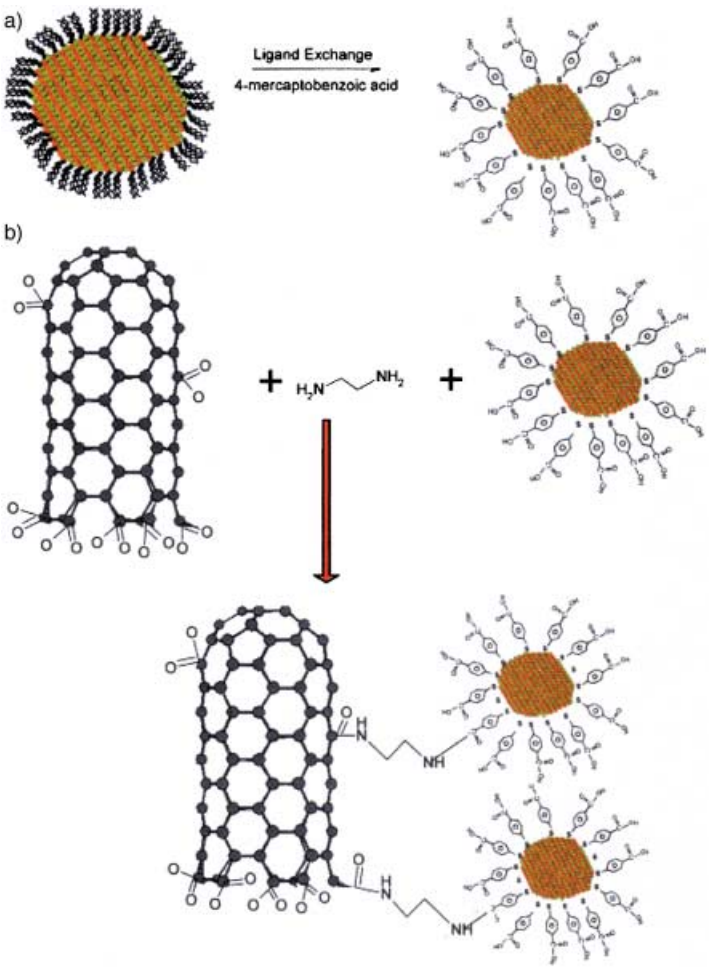

Figure 9. Schematic diagram of the addition of CdSe nanocrystals to oxidized SWNTs. TOPO capped nanocrystals were prepared by established methods using organometallic precursors. a) TOPO capping was substituted for a thiol ligand to form a carboxylic acid-terminated CdSe nanocrystal. Substituted thiocarboxylic acids used included *p*-mercaptobenzoic acid, thioglycolic acid, and 3-mercaptopropionic acid. b) The nanocrystals prepared in a) were linked to oxidized SWNTs by an ethylenediamine linker in the presence of EDC.

to the nanotube in the CdSe–nanotube system, whereas in the TiO_2–nanotube system, charge transfer is expected to occur from tube to nanocrystal. Further studies with the TiO_2–nanotube system will lead to an understanding of charge transfer properties with potential in solar cell applications.[65]

TEM examination (Figure 10) showed nanocrystals linked to the oxidized SWNTs, forming discrete nanocomposites. The nanocrystals tend to be concentrated at the open caps and

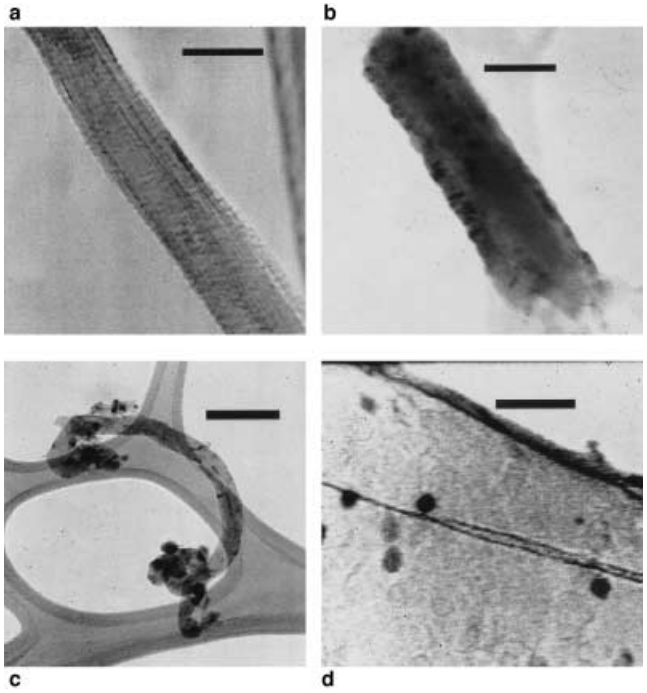

Figure 10. TEMs of a) a purified single-walled carbon nanotube bundle (scale bar denotes 30 nm), b) oxidized SWNT bundle circumscribed by capped TiO_2 particles (scale bar is 45 nm), c) oxidized tubes linked to CdSe nanocrystals capped with 4-mercaptobenzoic acid (the crystallites are concentrated at the functionalized open ends, with some coverage on the sidewalls, likely at defect sites; scale bar is 150 nm), d) oxidized nanotube linked to CdSe nanoparticles capped with 3-mercaptopropionic acid (image at high magnification shows prolate nanocrystals scattered along the length of the tube; scale bar represents 20 nm).

the "ends", where there is the largest concentration of carboxylic groups[66, 67] and, thus, the highest probability of amide bond formation.[27] A commonly observed structure was a cluster of nanoparticles, especially in the case of CdSe, localized at the outer edges of the tubes (Figure 10c). In other cases, especially with longer and thinner tubes, numbers of nanocrystals tended to disperse along the sidewalls, presumably attaching to defect sites on the oxidized nanotube surface (Figure 10d). The TiO_2 system showed substantially greater coverage of the tubes with the nanoparticles (Figure 10b). Carboxyl groups adsorb strongly onto bare titanium dioxide surfaces.[68] Hence, larger numbers of these particles can interact with nanotubes and, in effect, amide bond formation may not be required for an underivatized, uncapped TiO_2–SWNT adduct to be directly produced. Indeed, we postulate that this is the reason for enhanced coverage with TiO_2 particles. EDX analysis on both nanocomposite systems was consistent with the presence of appropriately functionalized nanocrystals attached to nanotubes as proposed.

These patterns of nanocrystal clustering on the nanotubes were not observed in control experiments, without the use of carbodiimide linking agents, whereby the tubes themselves were found to remain totally separate from the nanocrystals. Hence, the significance of this work is that wet solution functionalization techniques, especially with the quantum dots and oxide nanocrystals, provide us with a degree of spatial control at the nanoscale level, with regard to the location of chemical derivatization on the surfaces of these tubes, depending on the linker and capping agent used.

Conclusions

Rational nanotube functionalization allows for the manipulation of nanoscale properties in a predictive manner. In this article, we have described a variety of molecular organic- and inorganic-inspired methodologies to chemically modify nanotube structures, including metal coordination, solution-phase ozonolysis, and the formation of nanotube–nanocrystal heterostructures.

Derivatization of oxidized SWNTs with metal-containing molecular complexes, such as Vaska's and Wilkinson's complexes, renders them soluble and stable in a variety of different organic solvents, including traditionally poor ones for nanotubes, thereby enabling further exploitation of their wet chemistry. The chemical functionalization reaction occurs through the creation of a metal–oxygen bond and results in exfoliation of larger nanotube bundles, creating an increased distribution of smaller diameter tubes. Moreover, as the tubes are readily recoverable from solution, this finding has significant scientific and economic implications for nanotubes as reusable catalyst supports, particularly for expensive catalyst materials. We expect similar types of nanotube coordination chemistry to be seen with other molecular complexes. Indeed, molecular metal complexation with nanotubes may not only provide the basis for site-selective nanochemistry and self-assembly applications, but also enable a means of altering the known electronic, optical, and mechanical properties of SWNTs in a controllable manner.

Chemical functionalization of the sidewalls of SWNTs, through ozonolysis in solution, not only conserves the structural integrity of the tube bundles, but also purifies them, removing a large number of metal impurities and amorphous carbon entities. Significantly, this work bears out the theoretical prediction that 1,3-dipolar cycloaddition to the SWNT sidewalls is experimentally achievable. In fact, these experiments indicate that a certain degree of control over the presence of particular functional groups on the surfaces of these SWNTs can be obtained by judicious choice of the appropriate cleaving agent of the ozonide intermediate, all of which can be achieved with minimal sample loss. More importantly, this protocol presents a nondestructive, low-temperature method of introducing oxygenated functionalities directly onto the sidewalls and not simply at the end caps of SWNTs. Thus, molecular species, which can be currently tethered to the ends of the nanotubes, can now also be

chemically dispersed along the sidewalls, with implications for the design of well-dispersed nanotube-based composites. We are currently exploring similar types of cycloaddition reactions to SWNT, as these are expected to shed considerable light on the nature of the conjugated C=C bonds in these structures.

Our synthesis of novel nanotube–nanocrystal nanostructure composites, involving chalcogenide and metal oxide nanocrystals, is another promising means of creating both physically and chemically configurable nanomaterials. Generating such a nanoscale heterojunction, incorporating both nanocrystals and SWNTs into a single covalently linked heterostructure, is significant not only because no such device has been reported previously, but also because interesting charge-transfer behavior is conceivable across the nanotube–nanocrystal interface. As such, the efficiency of charge separation and recombination in such systems can be conveniently tuned by varying the size, shape, and chemistry, of nanotubes and nanocrystals and also the donor–acceptor distance between them. In other words, we are creating a sharp junction interface, whose properties are manipulable and, hence, predictable. The implication is that the direction of charge and electron transfer as well as the longevity of such light- and potential-induced charge separation can be modulated; this of course is of importance to the development of photoelectrochromic materials, in particular optical storage devices.

Because all of our studies also show the potential for novel charge transfer characteristics in these functionalized materials, the development and understanding of these derivatized structures have implications also for molecular electronics, photocatalysis, and for scanning probe microscopy with functionalized tips.

Acknowledgements

We acknowledge support of this work through startup funds provided by the State University of New York at Stony Brook as well as Brookhaven National Laboratory. Acknowledgement is also made to the donors of the Petroleum Research Fund, administered by the American Chemical Society, for support of this research. We also thank Dr. James Marecek and Dr. James Quinn for their guidance with the NMR and SEM/TEM work, respectively. S.S.W. also thanks 3M for a Nontenured Faculty Award.

[1] A. Thess, R. Lee, P. Nikolaev, H. Dai, P. Petit, J. Robert, C. Xu, Y. H. Lee, S. G. Kim, A. G. Rinzler, D. T. Colbert, G. E. Scuseria, D. Tomanek, J. E. Fischer, R. E. Smalley, *Science* **1996**, *273*, 483–487.
[2] M. S. Dresselhaus, G. Dresselhaus, P. Avouris, *Carbon Nanotubes Synthesis, Structure, Properties, and Applications*, Springer, Berlin, **2001**.
[3] S. Saito, *Science* **1997**, *278*, 77–78.
[4] M. R. Falvo, G. J. Clary, R. M. I. Taylor, V. Chi, F. P. J. Brooks, S. Washburn, R. Superfine, *Nature* **1997**, *389*, 582–584.
[5] T. W. Odom, J.-L. Huang, P. Kim, C. M. Lieber, *Nature* **1998**, *391*, 62–64.
[6] A. Bachtold, P. Hadley, T. Nakanshi, C. Dekker, *Science* **2001**, *294*, 1317–1320.
[7] V. Lordi, N. Yao, J. Wei, *Chem. Mater.* **2001**, *13*, 733–737.
[8] J. M. Planeix, N. Coustel, B. Coq, P. M. Ajayan, *J. Am. Chem. Soc.* **1994**, *116*, 7935–7936.
[9] R. H. Baughman, C. Cui, A. A. Zakhidov, Z. Iqbal, J. N. Barisci, G. M. Spinks, G. G. Wallace, A. Mazzoldi, D. De Rossi, A. G. Rinzler, O. Jachinski, S. Roth, M. Kertesz, *Science* **1999**, *284*, 1340–1344.
[10] R. H. Baughman, A. A. Zakhidov, W. A. de Heer, *Science* **2002**, *297*, 787–792.
[11] S. Fan, M. G. Chapline, N. R. Franklin, T. W. Tombler, A. M. Cassell, H. Dai, *Science* **1999**, *283*, 512–514.
[12] W. Zhao, C. Song, P. E. Pehrsson, *J. Am. Chem. Soc.* **2002**, *124*, 12418–12419.
[13] J. Kong, N. R. Franklin, C. Zhou, M. G. Chapline, S. Peng, K. Cho, H. Dai, *Science* **2000**, *287*, 622–625.
[14] C.-M. Yang, K. Kaneko, M. Yudasaka, S. Iijima, *Nano Lett.* **2002**, *2*, 385–388.
[15] S. S. Wong, J. D. Harper, P. T. Lansbury, C. M. Lieber, *J. Am. Chem. Soc.* **1998**, *120*, 603–604.
[16] A. Hirsch, *Angew. Chem.* **2002**, *114*, 1933–1939; *Angew. Chem. Int. Ed.* **2002**, *41*, 1853–1859.
[17] S. B. Sinnott, *J. Nanosci. Nanotech.* **2002**, *2*, 113–123.
[18] J. Bahr, J. M. Tour, *J. Mater. Chem.* **2002**, *12*, 1952–1958.
[19] V. Georgakilas, K. Kordatos, M. Prato, D. M. Guldi, M. Holzinger, A. Hirsch, *J. Am. Chem. Soc.* **2002**, *124*, 760–761.
[20] J. L. Bahr, J. Yang, D. V. Kosynkin, M. J. Broniskowski, R. E. Smalley, J. M. Tour, *J. Am. Chem. Soc.* **2001**, *123*, 6536–6542.
[21] E. T. Mickelson, C. B. Huffman, A. G. Rinzler, R. E. Smalley, R. H. Hauge, J. L. Margrave, *Chem. Phys. Lett.* **1998**, *296*, 188–194.
[22] R. J. Chen, Y. Zhang, D. Wang, H. Dai, *J. Am. Chem. Soc.* **2001**, *123*, 3838–3339.
[23] J. Chen, M. A. Hamon, H. Hu, Y. Chen, A. M. Rao, P. C. Eklund, R. C. Haddon, *Science* **1998**, *282*, 95–98.
[24] M. O'Connell, P. Boul, L. M. Ericson, C. Huffman, Y. Wang, E. Haroz, C. Kuper, J. Tour, K. D. Ausman, R. E. Smalley, *Chem. Phys. Lett.* **2001**, *342*, 265–271.
[25] J. E. Riggs, Z. Guo, D. L. Carroll, Y.-P. Sun, *J. Am. Chem. Soc.* **2000**, *122*, 5879–5880.
[26] A. Star, J. F. Stoddart, D. Steurman, M. Diehl, A. Boukai, E. W. Wong, X. Yang, S.-W. Chung, H. Choi, J. R. Heath, *Angew. Chem.* **2001**, *113*, 1771–1775; *Angew. Chem. Int. Ed.* **2001**, *40*, 1721–1725.
[27] S. S. Wong, E. Joselevich, A. T. Woolley, C. L. Cheung, C. M. Lieber, *Nature* **1998**, *394*, 52–55.
[28] S. S. Wong, A. T. Woolley, E. Joselevich, C. L. Cheung, C. M. Lieber, *J. Am. Chem. Soc.* **1998**, *120*, 8557–8558.
[29] S. Niyogi, H. Hu, M. A. Hamon, P. Bhowmik, B. Zhao, S. M. Rozenhak, J. Chen, M. E. Itkis, M. S. Meier, R. C. Haddon, *J. Am. Chem. Soc.* **2001**, *123*, 733–734.
[30] B. Zhao, H. Hu, S. Niyogi, M. E. Itkis, M. A. Hamon, P. Bhowmik, M. S. Meir, R. C. Haddon, *J. Am. Chem. Soc.* **2001**, *123*, 11673–11674.
[31] B. Z. Tang, H. Xu, *Macromolecules* **1999**, *32*, 2569–2576.
[32] J. L. Bahr, E. T. Mickelson, M. J. Bronikowski, R. E. Smalley, J. M. Tour, *Chem. Commun.* **2001**, 193–194.
[33] F. Pompeo, D. E. Resasco, *Nano Lett.* **2002**, *2*, 369–373.
[34] R. Bandyopadhyaya, E. Nativ-Roth, O. Regev, R. Yerushalmi-Rozen, *Nano Lett.* **2002**, *2*, 25–28.
[35] S. Banerjee, S. S. Wong, *Nano Lett.* **2002**, *2*, 49–55.
[36] Y. S. Sohn, A. L. Balch, *J. Am. Chem. Soc.* **1972**, *94*, 1144–1148.
[37] F. Nunzi, F. Mercuri, A. Sgamellotti, N. Re, *J. Phys. Chem. B* **2002**, *106*, 10622–10633.
[38] R. Brady, B. R. Flynn, G. L. Geoffroy, H. B. Gray, J. J. Peone, L. Vaska, *Inorg. Chem.* **1976**, *15*, 1485–1488.
[39] A. Hirsch, *Chemistry of the Fullerenes*, Thieme, Stuttgart, **1994**.
[40] R. Taylor, D. R. M. Walton, *Nature* **1993**, *363*, 685–693.
[41] R. C. Haddon, *Science* **1993**, *261*, 1545–1550.
[42] R. C. Haddon, *Acc. Chem. Res.* **1988**, *21*, 243–249.
[43] M. A. Hamon, M. E. Itkis, S. Niyogi, T. Alvaraez, C. Kuper, M. Menon, R. C. Haddon, *J. Am. Chem. Soc.* **2001**, *123*, 11292–11293.
[44] W. Zhou, Y. H. Ooi, R. Russo, P. Papanek, D. E. Luzzi, J. E. Fischer, M. J. Bronikowski, P. A. Willis, R. E. Smalley, *Chem. Phys. Lett.* **2001**, *350*, 6–14.
[45] N. Wang, Z. K. Tang, G. D. Li, J. S. Chen, *Nature* **2000**, *408*, 50–51.
[46] S. Banerjee, S. S. Wong, *J. Am. Chem. Soc.* **2002**, *124*, 8940–8948.
[47] J. L. Bahr, J. M. Tour, *Chem. Mater.* **2001**, *13*, 3823–3824.
[48] K. D. Ausman, R. Piner, O. Lourie, R. S. Ruoff, M. Korobov, *J. Phys. Chem. B* **2000**, *104*, 8911–8915.

[49] J. Chen, A. M. Rao, S. Lyuksyutov , M. E. Itkis, M. A. Hamon, H. Hu, R. W. Cohn, P. C. Eklund, D. T. Colbert, R. E. Smalley, R. C. Haddon, *J. Phys. Chem. B* **2001**, *105*, 2525 – 2528.
[50] M. J. O'Connell, S. M. Bachilo, C. B. Huffman, V. C. Moore, M. S. Strano, E. H. Haroz, K. L. Rialon, P. J. Poul, W. H. Noon, C. Kittrell, J. Ma, R. H. Hauge, B. R. Weisman, R. E. Smalley, *Science* **2002**, *297*, 593 – 596.
[51] O. Jost, A. A. Gorbunov, W. Pompe, T. Pickler, R. Friedlein, M. Kupfer, M. Reibold, H.-D. Bauer, L. Dunsch, M. S. Golden, J. Fink, *Appl. Phys. Lett.* **1999**, *75*, 2217 – 2219.
[52] J. W. G. Wildoer, L. C. Venema, A. G. Rinzler, R. E. Smalley, C. Dekker, *Nature* **1998**, *391*, 59 – 62.
[53] H. Kataura, Y. Kumazawa, Y. Maniwa, I. Umezu, S. Suzuki, Y. Ohtsuka, Y. Achiba, *Synth. Met.* **1999**, *103*, 2555 – 2558.
[54] F. Frehill, J. G. Vos, S. Benrezzak, A. A. Koos, Z. Konya, M. G. Ruther, W. J. Blau, A. Fonseca, J. B. Nagy, L. P. Biro, A. I. Minett, M. in Het Panhuis, *J. Am. Chem. Soc.* **2002**, *124*, 13694 – 13695.
[55] M. G. C. Kahn, S. Banerjee, S. S. Wong, *Nano Lett.* **2002**, *2*, 1215 – 1218.
[56] S. Banerjee, S. S. Wong, *J. Phys. Chem. B* **2002**, *106*, 12144 – 12151.
[57] L. B. Harding, W. A. Goddard III, *J. Am. Chem. Soc.* **1978**, *100*, 7180 – 7188.
[58] W. H. Lee, S. J. Kim, W. J. Lee, J. G. Lee, R. C. Haddon, P. J. Reucroft, *Appl. Surf. Sci.* **2001**, *181*, 121 – 127.
[59] H. Hiura, T. W. Ebbesen, K. Tanigaki, *Adv. Mater.* **1995**, *7*, 275 – 276.
[60] D. B. Mawhinney, V. Naumenko, A. Kuznetsova, J. T. Yates, Jr., J. Liu, R. E. Smalley, *J. Am. Chem. Soc.* **2000**, *122*, 2383.
[61] L. E. Brus, *Appl. Phys. A* **1991**, *53*, 465 – 474.
[62] B. O. Dabbousi, J. Rodriguez-Viejo, F. V. Mikulec, J. R. Heine, H. Mattoussi, R. Ober, K. F. Jensen, M. G. Bawendi, *J. Phys. Chem. B* **1997**, *101*, 9463 – 9475.
[63] A. P. Alivisatos, *J. Phys. Chem.* **1996**, *100*, 13226 – 13239.
[64] S. Banerjee, S. S. Wong, *Nano Lett.* **2002**, *2*, 195 – 200.
[65] K.-H. Jung, J. S. Hong, R. Vittal, K.-J. Kim, *Chem. Lett.* **2002**, *8*, 864 – 865.
[66] P. M. Ajayan, T. W. Ebbesen, T. Ichihashi, S. Iijima, K. Tanigaki, H. Hiura, *Nature* **1993**, *361*, 333 – 334.
[67] J. Liu, A. G. Rinzler, H. Dai, J. H. Hafner, R. K. Bradley, P. J. Boul, A. Lu, T. Iverson, K. Shelimov, C. B. Huffman, F. Rodriguez-Macias, Y. S. Shon, T. R. Lee, D. T. Colbert, R. E. Smalley, *Science* **1998**, *280*, 1253 – 1256.
[68] D. Lawless, S. Kapoor, D. Meisel, *J. Phys. Chem.* **1995**, *99*, 10329 – 10335.